



# HHS Public Access

Author manuscript

*Conf Proc IEEE Eng Med Biol Soc.* Author manuscript; available in PMC 2017 September 05.

Published in final edited form as:

*Conf Proc IEEE Eng Med Biol Soc.* 2011 ; 2011: 7470–7473. doi:10.1109/IEMBS.2011.6091843.

## Predicting Efficacy of Robot-Aided Rehabilitation in Chronic Stroke Patients using an MRI-Compatible Robotic Device

**Fabrizio Sergi [Student Member, IEEE],**

Università Campus Bio-Medico di Roma, Center for Integrated research, Laboratory of Biomedical Robotics and Biomicrosystems, Rome, Italy

**Hermano Igo Krebs [Senior Member, IEEE],**

Massachusetts Institute of Technology, Mechanical Engineering Department, Cambridge, MA 02139 USA and University of Maryland School of Medicine, Neurology Department, Baltimore, MD 21201

**Benjamin Groissier,**

Massachusetts General Hospital, Martinos Center for Biomedical Imaging, Neurorecovery Laboratory

**Avrielle Rykman,**

Burke Medical Research Institute, White Plains, NY

**Eugenio Guglielmelli [Senior Member, IEEE],**

Università Campus Bio-Medico di Roma, Center for Integrated research, Laboratory of Biomedical Robotics and Biomicrosystems, Rome, Italy

**Bruce T. Volpe, and**

Burke Medical Research Institute, White Plains, NY

**Judith D. Schaechter**

Massachusetts General Hospital, Martinos Center for Biomedical Imaging, Neurorecovery Laboratory

### Abstract

We are investigating the neural correlates of motor recovery promoted by robot-mediated therapy in chronic stroke. This pilot study asked whether efficacy of robot-aided motor rehabilitation in chronic stroke could be predicted by a change in functional connectivity within the sensorimotor network in response to a bout of motor rehabilitation. To address this question, two stroke patients participated in a functional connectivity MRI study pre and post a 12-week robot-aided motor rehabilitation program. Functional connectivity was evaluated during three consecutive scans before the rehabilitation program: resting-state; point-to-point reaching movements executed by the paretic upper extremity (UE) using a newly developed MRI-compatible sensorized passive manipulandum; resting-state. A single resting-state scan was conducted after the rehabilitation program. Before the program, UE movement reduced functional connectivity between the

---

H.I.K is a co-inventor in MIT-held patent for the robotic devices used to delivered therapy. He holds equity positions in Interactive Motion Technologies, Inc., the company that manufactures this type of technology under license to MIT.

ipsilesional and contralesional primary motor cortex. Reduced interhemispheric functional connectivity persisted during the second resting-state scan relative to the first and during the resting-state scan after the rehabilitation program. Greater reduction in interhemispheric functional connectivity during the resting-state was associated with greater gains in UE motor function induced by the 12-week robotic therapy program. These findings suggest that greater reduction in interhemispheric functional connectivity in response to a bout of motor rehabilitation may predict greater efficacy of the full rehabilitation program.

---

## I. Introduction

EACH year in the United States, about 795,000 adults experience a stroke, most often resulting in hemiparesis.

While some motor recovery typically occurs over the subsequent months, about 50% of stroke patients are left with residual motor deficits [1]. Several motor rehabilitation approaches are currently available: among these, robot-aided rehabilitation has been shown to effectively improve motor function of the paretic upper extremity (UE) [2]. Nevertheless, the efficacy of robot-aided rehabilitation, and motor rehabilitation approaches in general, has a high degree of inter-subject variability, such that differences in treatment efficacy among stroke patients are not well predicted by variables such as time after stroke, age or severity of baseline motor deficit. However, it is possible that the efficacy of a particular motor rehabilitation may be predicted using functional neuroimaging. Indeed, recent functional neuroimaging studies in stroke patients have suggested that efficacy of a motor rehabilitation can be predicted by the response of the sensorimotor network (SMN) to a motor challenge [3] [4].

Functional connectivity MRI (fcMRI) is a relatively new functional neuroimaging technique, which measures the strength of correlations between brain regions in the low-frequency components of the blood oxygen level-dependent (BOLD) signal, and is believed to reflect direct or indirect synaptic connections [5]. When healthy normal adults are not engaged in a particular task (condition called resting state), fcMRI has shown that the low-frequency BOLD signals in the right and left SMN are highly correlated [5]. Strikingly, when healthy normal adults perform unilateral UE movements, there is a marked reduction in the functional connectivity between both hemispheres sensorimotor regions [6]. Functional connectivity within the SMN is also modulated by prior activity, such as motor learning [7].

In this exploratory, pilot study, we asked if the efficacy of robot-aided rehabilitation in chronic stroke patients could be predicted by the change in functional connectivity within the SMN in response to a bout of robot-aided rehabilitation. To address this question, we conducted an fcMRI study in stroke patients just prior to and after they participated in a 12-week program of robot-aided rehabilitation. This study utilized a newly developed MRI-compatible sensorized passive manipulandum that visually prompted the execution of point-to-point reaching movements similar to those used during the robot-aided rehabilitation program.

## II. Materials and Methods

### A. Study design and subjects

Two patients with chronic hemiparesis enrolled in this pilot study (Table I). Patients participated in a 12-week, 3 times per week, program of robot-aided rehabilitation therapy at the Burke Rehabilitation Hospital, White Plains, NY. The robot-aided therapy used the InMotion2 shoulder-elbow robot and the InMotion3 wrist robot (Interactive Motion Technologies, Watertown, MA) [8] [9]. Before and after the 12-week therapy program, the patients underwent motor function testing and MRI.

In addition, two healthy normal adults participated to one MRI session in order to determine brain regions normally activated during UE movement when interacting with the MRI-compatible robotic device. These data were used for analysis of fMRI data acquired from patients.

### B. Motor function testing

Motor function testing was administered by a licensed physical therapist. The following tests were conducted: 1) UE motor section of the Fugl-Meyer (FM) Stroke Scale, providing an overall measure of motor impairment (scale 0–66, 66 = normal); 2) Medical Research Council (MRC) scale to measure strength of 18 UE muscles (scale 0–90; full strength of all muscles = 90); 3) Hand grip strength using a digital dynamometer (mean of peak,  $2 \times 5$ -s trials), with paretic grip strength normalized (in percent) to that of the opposite hand [10].

### C. MRI-compatible passive manipulandum

A passive planar 2-degree-of-freedom parallelogram manipulandum was developed as an MRI-compatible equivalent of the shoulder and elbow robot [8], used during robot-aided rehabilitation therapy sessions. The base of the device was made of wood; it conformed to the lumbar spine curvature while the subject lied supine, with the subject's weight anchoring the device during manipulation. Most of the remaining structure, including post, platform and manipulandum arms, was made of Delrin. To guarantee low friction, we employed off-the-shelf plastic ball bearings with glass balls. These bearings cannot take vertical loading and hence the device includes a horizontal platform that is positioned under the handle and unloads the weight of the subject's arm. To minimize friction between the handle and platform, we made the handle of Teflon.

Two MRI compatible fiber-optics angle sensors (S700, Measurand Inc.) were used to measure the rotation of the two distal links relative to the ground frame ( $\theta_1, \theta_2$ ). The sensors consist of an optic fiber, whose light beam (intensity decrease proportional to fiber curvature and thus to links angle) was sent over an additional 10-meter optical fiber to send the signal out of the room housing the MRI scanner and converted into an analogue voltage. Since all links were of equal length  $l$ , the forward kinematics, described by the planar coordinates of the robot handle ( $x_h, y_h$ ) could be computed through the simple forward kinematics formula:

$$\begin{cases} x_h = l \cdot \cos(\theta_1) + l \cdot \cos(\theta_2) \\ y_h = l \cdot \sin(\theta_1) + l \cdot \sin(\theta_2) \end{cases} \quad 1)$$

The handle position was measured at 1 kHz and displayed in real-time to the subject through a mirror projection system, in a graphical user interface (GUI) resembling the “clock” game employed during the 12-week robot-aided rehabilitation [8].

To minimize head movement and body mass movement during MRI, which can result in BOLD signal artifacts, [11], UE movement length was limited to 4 cm and only to half of the clock game directions, as already suggested in [12].

The GUI prompted the execution of point-to-point reaching movements with targets presented randomly every 3.2 s, alternating between the center target and a periphery target. Visual cues were provided to guide reaching movements lasting about 1.6 s. Subjects were trained briefly prior to MRI. All subjects found the GUI clear and intuitive.

#### D. Kinematic analysis of UE movement during MRI

The planar coordinates of the point-to-point reaching movements during MRI were analyzed to determine global indices of movement. The velocity vector  $\mathbf{v}_h(t)$  components were computed using a smoothing/derivative numerical filter (3<sup>rd</sup> order Savitzky-Golay, temporal window: 0.35 s). A threshold velocity value  $v_{th}$  was defined as 2% of peak velocity. Movement duration was then calculated by measuring the temporal interval corresponding to the time-frames  $t_i$  respecting the condition  $|\mathbf{v}_h(t_i)| > v_{th}$ . Displacement was calculated by numerical integration of the velocity profile over time.

#### E. Image acquisition

Images were acquired at the Massachusetts General Hospital, Martinos Center for Biomedical Imaging using a 3T Siemens TIM Trio MRI scanner with a 12-channel head coil.

For patients, three BOLD scans were acquired in succession before the 12-week robot-aided rehabilitation program and one BOLD scan was acquired after the program. BOLD images were collected using a T<sub>2</sub>\*-weighted gradient echo, echo planar imaging sequence (repetition time [TR]=2 s; echo time [TE]=30 ms, flip angle [α]=90°, field-of-view [FOV]=220 × 220 mm; matrix size=72 × 72, in-plane resolution=3.125 mm, slice thickness=4 mm, interslice distance=0.8 mm, number of slices=32, number of acquisition/slice=180; scan duration=6 min) that was equipped with real-time correction for head motion [13]. At the pre-therapy MRI session, the first and third BOLD scans were collected during the resting-state, when subjects were instructed to visually fixate a crosshair. During acquisition of the intervening, second BOLD scan, patients were instructed to move their paretic (left) UE as prompted by the GUI (i.e., to perform a point-to-point reaching movement every 3.2 s), for a total of 180 s of prompted movement and 180 s of rest.

A high-resolution structural scan was also collected at both sessions using a multi-echo magnetization prepared rapid gradient echo (MEMPR) sequence [14]. Fluid attenuated inversion recovery images were acquired to provide anatomical localization of the lesion.

For normal subjects, a single BOLD scan was acquired using the same parameters as described above with the exception that the number of acquisitions/slice was 150 and the scan duration was 5 minutes. During this BOLD scan, subjects alternated between moving the left UE in response to the GUI ( $4 \times 32$  s) and a control condition ( $5 \times 32$  s). During the control condition, subjects were instructed to visually track movements (without UE movement) of the cursor that moved along a straight minimum-jerk trajectory between the center target and a periphery target.

## F. Image analysis

Preprocessing and statistical analysis of functional images was performed using AFNI [15] and FSL [16] software. BOLD data from normal subjects were slice-time and motion corrected; signal intensity normalized; and de-noised using an Independent Component Analysis-based algorithm [17]. Data were spatially smoothed using a Gaussian kernel with a full-width at half maximum (FWHM) of 6 mm. A voxel-wise general linear model (GLM) was constructed which included a stimulus input function defined as the sequence of movement and control conditions in a boxcar function convolved with a canonical hemodynamic response. The resultant z-statistic map was registered nonlinearly to the MNI152 standard brain space and averaged between the two normal subjects. The average z-statistic map was thresholded to a Bonferroni-corrected  $p$  value of 0.05, and then segmented on a functional-anatomical basis. The 50 contiguous voxels exhibiting the most significant activation response in the right primary motor cortex (M1) during left UE movement were identified. This was accomplished using a recursive algorithm starting from the centroid of the average z-statistic map within the Brodmann area 4 defined by the Juelich Histological Atlas [18] in MNI152 brain space (Fig. 1). This 50-voxel region within the right M1 was utilized in the analysis of fMRI data acquired from patients.

Each of the BOLD scans acquired from patients were slice-time and motion corrected, and then registered nonlinearly to the MNI152 standard brain space. The data were spatially smoothed with a Gaussian kernel (FWHM= 6 mm) and bandpass filtered (FWHM cut-off frequencies of 0.008 and 0.1 Hz). A GLM was constructed which included the mean BOLD time-series extracted from the seed region in the right M1 (i.e., the 50-voxel region defined in normal subjects as maximally active during left UE movement) as the regressor-of-interest. Nine nuisance regressors were also included in the GLM in order to remove sources of spurious variance: i) six parameters of the rigid body transformation estimated by the motion correction algorithm, ii) the mean whole-brain BOLD time-series, iii) mean BOLD time-series in brain white matter; iv) mean BOLD time-series in the lateral ventricles. For each patient, voxels in the lesion were excluded from computation of regressor time-series and functional connectivity maps. To quantify the strength of interhemispheric connectivity between the seed region in the right (ipsilesional) and the target-of-interest in the left (contralesional) M1, the mean z-statistic in the lateral portion of left Brodmann area 4 [18] was calculated.

### III. Results

Before initiation of the 12-week robot-aided rehabilitation program, the first resting-state scan showed strong functional connectivity between the seed region in the right (ipsilesional) M1 and many regions of the SMN, including the target-of-interest in the left (contralesional) M1 (Figs. 2 and 3).

Point-to-point reaching movements with the paretic (left) UE reduced functional connectivity between the right M1 seed region and many SMN regions of the left hemisphere, including the left target-of-interest. Patient 1 showed greater reduction in functional connectivity between the seed and target regions as a result of the point-to-point movements compared to Patient 2. Kinematic analysis of the point-to-point movements showed that movement duration and displacement were greater in Patient 1 than Patient 2 (Table II). The second resting-state scan that immediately followed the UE movement scan showed that Patient 1 largely retained the reduction in functional connectivity between the right and left M1. In contrast, functional connectivity between the right and left M1 largely reverted to the high level observed during the first resting-state scan in Patient 2 (Fig 2). After completion of the 12-week program, resting-state functional connectivity between the seed region in the right M1 and regions of the SMN in the left hemisphere, including the target-of-interest in M1, remained relatively low in Patient 1 and similar to the level during the pre-therapy, resting-state scan immediately following UE movement. Patient 2, in contrast, showed that functional connectivity between the seed and target regions during the resting-state scan was similar to that observed during the two pre-therapy resting-state scans. Motor function testing showed that Patient 1 made greater gains in the FM, MRC and grip strength compared to Patient 2 (Table III). Therefore, the efficacy of the robot-aided rehabilitation as well as the magnitude of change in functional connectivity between the right and left M1 in response to the bout of the rehabilitation was greater in Patient 1 compared to Patient 2.

### IV. Discussion and conclusions

This exploratory pilot study asked if efficacy of a 12-week robot-aided rehabilitation program in two stroke patients with chronic hemiparesis could be predicted by a change in functional connectivity within the SMN in response to a bout of the robot-aided rehabilitation. Functional connectivity between the ipsilesional and contralesional M1 was measured using fcMRI. An MRI-compatible robotic device was built and employed to deliver the bout of robot-aided rehabilitation during MRI. We found that Patient 1, compared to Patient 2, made both greater gains in motor function of the paretic UE after the 12-week program and exhibited a greater reduction in functional connectivity between the ipsilesional and contralesional M1 in response to the bout of rehabilitation. Functional connectivity MRI appears to have been sensitive to differences in malleability of the SMN in response to robot-aided rehabilitation. These findings provide preliminary support of the concept that fcMRI may be useful in predicting efficacy of motor rehabilitation in chronic stroke patients.

Previous studies have suggested that motor recovery after stroke is promoted by a reduction in the inhibitory influence of the contralesional M1 on the ipsilesional M1 [19]. We

speculate that the observed reduction in functional connectivity between the M1s during the resting-state just after the bout of robot-aided rehabilitation and after the 12-week program may reflect a similar mechanism and may underlie gains in motor function after the robot-aided rehabilitation program.

Our preliminary observations of an association between the magnitude of change in functional connectivity after a bout of therapy and magnitude of motor function gain after a 12-week therapy program requires verification in a larger study. Future work may also evaluate the relative value of fcMRI, which provides a functional assessment of the SMN, to predict treatment efficacy, compared to structural assessments of the SMN (e.g., lesion volume and corticospinal tract damage). Such study could lead to the development of a multivariate prognostic model for predicting efficacy of a post-stroke rehabilitation.

## Acknowledgments

This work was supported in part by NIH grants # 1 R01-HD045343.

## References

1. Lloyd-Jones D, et al. Heart disease and stroke statistics--2010 update. A report from the American Heart Association. *Circulation*. 2009
2. Lo AC, et al. Robot-assisted therapy for long-term upper-limb impairment after stroke. *N Engl J Med*. 2010; 362(19):1772–83. [PubMed: 20400552]
3. Dong Y, Dobkin BH, Cen SY, Wu AD, Winstein CJ. Motor cortex activation during treatment may predict therapeutic gains in paretic hand function after stroke. *Stroke*. 2006;1552–1555. [PubMed: 16645139]
4. Cramer SC, et al. Predicting functional gains in a stroke trial. *Stroke*. 2007; 38(7):2108–2114. [PubMed: 17540966]
5. Biswal B, Yetkin F, Haughton VM, Hyde JS. Functional connectivity in the motor cortex of resting human brain using echo-planar MRI. *Magnet Reson Med*. 1995; 34(4):537–541.
6. Jiang T, He Y, Zhang Y, Weng X. Modulation of Functional Connectivity During the Resting State and the Motor Task. *Hum Brain Mapp*. 2004; 22:63–71. [PubMed: 15083527]
7. Albert NB, Robertson EM, Miall C. The resting human brain and motor learning. *Curr Biol*. 2009; 19(2):1023–1027. [PubMed: 19427210]
8. Krebs HI, Hogan N, Aisen ML, Volpe BT. Robot aided neurorehabilitation. *IEEE Trans on Rehab Eng*. 1998; 6(1):75–87.
9. Krebs HI, Volpe BT, Williams D, Celestino J, Charles SK, Lynch D, Hogan N. Robot-Aided Neurorehabilitation: A Robot for Wrist Rehabilitation. *IEEE Trans Neural Syst Rehab Eng*. 2007; 15(3):327–335.
10. Cramer SC, Nelles G, Schaechter JD, Kaplan JD, Finklestein SP. Computerized measurement of motor performance after stroke. *Stroke*. 1997; 28(11):2162.8. [PubMed: 9368558]
11. Diedrichsen J, Hashambhoy Y, Rane T, Shadmehr R. Neural correlates of reach errors. *J Neuroscience*. 2005; 25(43):9919–31. [PubMed: 16251440]
12. Krebs HI, Brashers-Krug T, Rauch SL, Savage CR, Hogan N, Rubin RH, Fischman AJ, Alpert NM. Robot-Aided Functional Imaging: Application to a Motor Learning Study. *Hum Brain Mapp*. 1998; 6:59–72. [PubMed: 9673663]
13. Thesen A, Heid O, Mueller E, Schad LR. Prospective acquisition correction for head motion with image-based tracking for real-time fMRI. *Magn Reson Med*. 2000; 44:457–465. [PubMed: 10975899]
14. van der Kouwe AJW, Benner T, Salat DH, Fischl B. Brain morphometry with multiecho MPRAGE. *Neuroimage*. 2008; 40(2):559–569. [PubMed: 18242102]

15. Cox RW. AFNI: software for analysis and visualization of functional magnetic resonance neuroimages. *Comput Biomed Res.* 1996; 29(3):162–173. [PubMed: 8812068]
16. Smith SM, et al. Advances in functional and structural MR image analysis and implementation as FSL. *Neuroimage.* 2004; 23:S208–19. [PubMed: 15501092]
17. Tohka J, Foerde K, Aron AR, Tom SM, Toga AW, Poldrack RA. Automatic Independent Component Labeling for Artifact Removal in fMRI. *NeuroImage.* 2008; 39(3):1227–45. [PubMed: 18042495]
18. Eickhoff SB, Stephan KE, Mohlberg H, Grefkes C, Fink GR, Amunts K, Zilles K. A new SPM toolbox for combining probabilistic cytoarchitectonic maps and functional imaging data. *Neuroimage.* 2005; 25(4):1325–35. [PubMed: 15850749]
19. Ward NS. Mechanisms underlying recovery of motor function after stroke. *Postgrad Med J.* 2005; 81:510–514. [PubMed: 16085742]



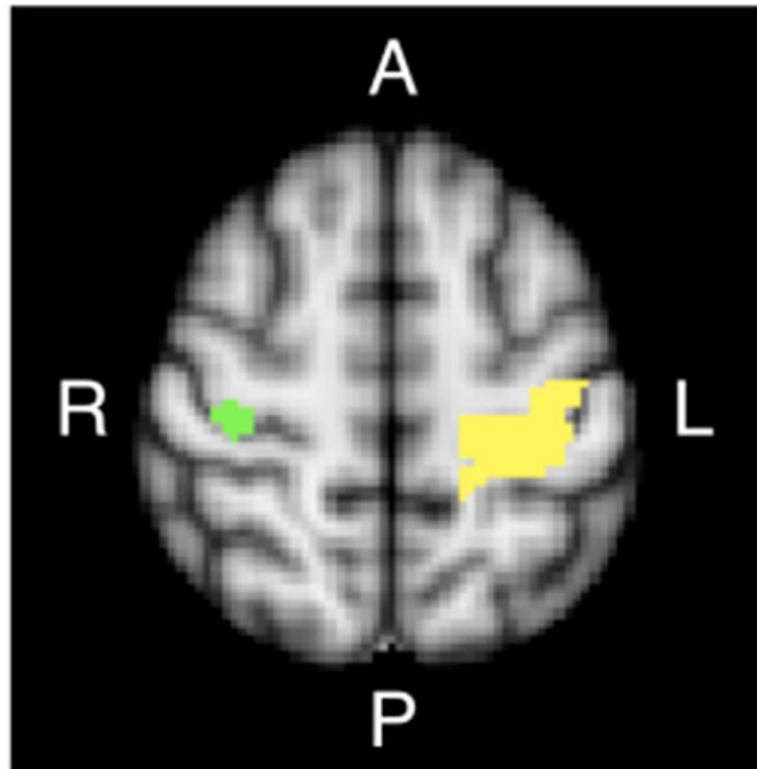


**Figure 1.** Seed region (green, in right M1) and target-of-interest (yellow, in left M1) applied in functional connectivity analysis, derived from fMRI conducted in normal adults while performing UE reaching movements. Regions were defined in MNI standard brain space (Axial slice,  $z = 58$  mm is shown).

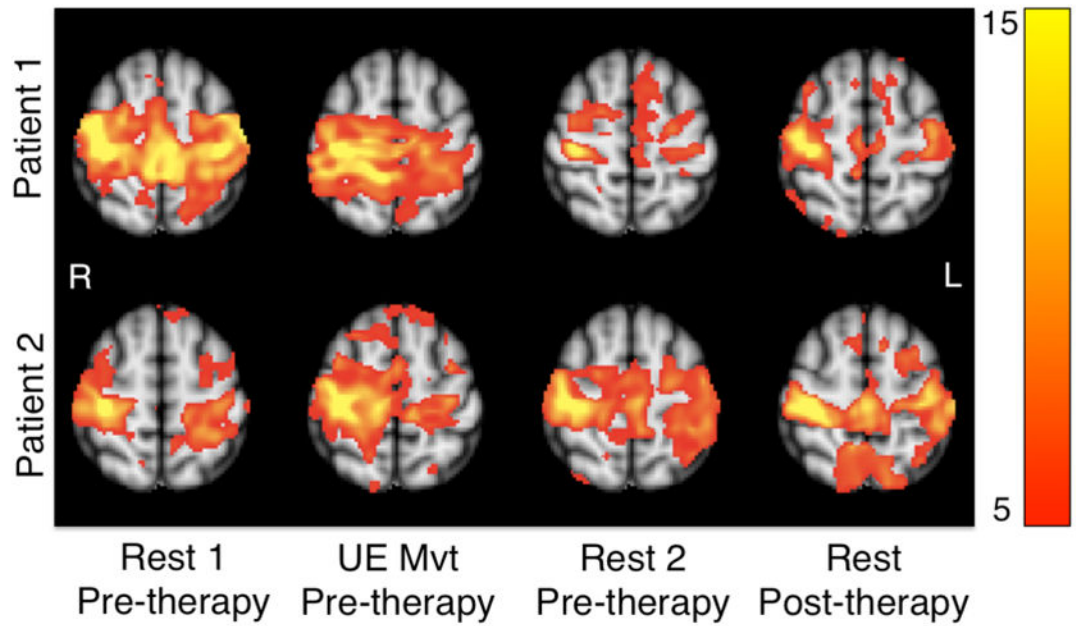


**Figure 2.**

Functional connectivity z-statistic maps (seed region in ipsilesional M1) in two patients before and after a 12-week robot-aided rehabilitation program. Before rehabilitation, two resting-state scans bounded a scan during which patients performed point-to-point movements guided by an MRI-compatible robotic device. After rehabilitation, patients participated in one resting-state scan. A single axial slice (MNI  $z = 58$ ) for each scan is shown.

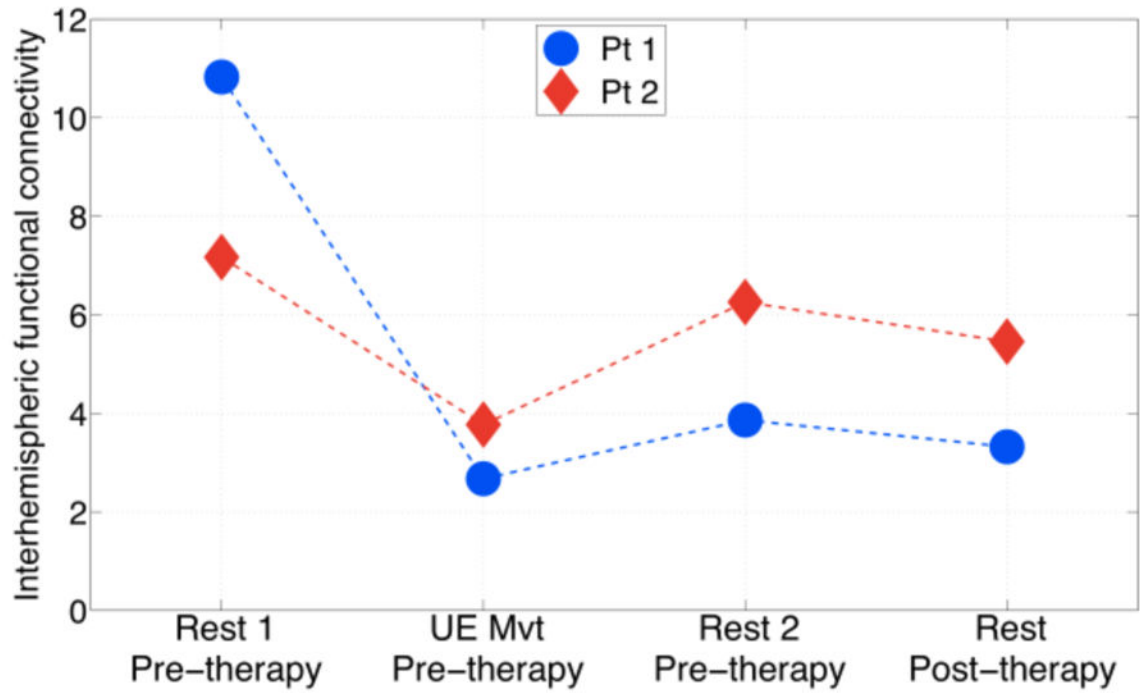


**Figure 3.** Interhemispheric functional connectivity between the right (ipsilesional) and left (contralesional) M1 in two patients. The metric of interhemispheric functional connectivity was the mean z-statistic in left M1.

Table 1

## PATIENTS CHARACTERISTICS

Patient #	Gender	Age [yr]	Time post-stroke [yr]	Handedness	Side of hemiparesis	Lesioned Hemisphere	Lesion Volume [cm <sup>3</sup> ]	Lesion Location
1	F	68	1.85	R	L	R	21	corona radiata, internal capsule, insula, putamen, globus pallidus
2	F	77	1.18	R	L	R	153	corona radiata, precentral gyrus, parietal lobe, insula, putamen; temporal lobe

**Table II**

kinematic indices of UE movement during fcMRI

Patient ID	Measured movement duration (prompted) [s]	Movement length [cm]
1	205 (180)	150
2	145 (180)	113

Author Manuscript

Author Manuscript

Author Manuscript

Author Manuscript

**Table III**

## Motor Function of Paretic UE

Test	Patient #	Pre-therapy	Post-therapy	Difference
FM score (0–66)	1	8	13	+5
	2	6	10	+4
MRC score (0–90)	1	21	36	+15
	2	24	30	+6
Grip (%contralateral hand)	1	1.5	11.1	+ 9.6
	2	0.6	6.2	+ 5.5

Author Manuscript

Author Manuscript

Author Manuscript

Author Manuscript